Differences between Collection 4 and 5 MODIS Ice Cloud Optical/Microphysical Products and their Impact on Radiative Forcing Simulations

Ping Yang, Lei Zhang, Gang Hong, Shaima L. Nasiri, Bryan A. Baum,
Hung-Lung Huang, Michael D. King, *Senior Member*, *IEEE*, and Steven Platnick

IEEE Transactions on Geoscience and Remote Sensing

Manuscript submitted December 2006, in final form February 2007

P. Yang, G. Hong, and S. L. Nasiri are with the Department of Atmospheric Sciences, Texas A&M University, College Station, TX 77843 USA (e-mail: pyang@ariel.met.tamu.edu).

L. Zhang was with the Department of Atmospheric Sciences, Texas A&M University when this study was carried out, and is now with the College of Atmospheric Sciences, Lanzhou University, Lanzhou 730000, China.

B. A. Baum and H. L. Huang are with Space Science and Engineering Center, University of Wisconsin-Madison, Madison, WI 53706 USA.

M. D. King and S. Platnick are with the Earth Sciences Division, NASA Goddard Space Flight Center, Greenbelt, MD 20771 USA.

Abstract—This paper reports on the comparison of two latest versions (Collection 4 and 5) of ice cloud products derived from the Moderate Resolution Imaging Spectroradiometer (MODIS) measurements. The differences between the bulk optical properties of ice clouds used in Collections 4 and 5 and the relevant impact on simulating the correlation of the bidirectional reflection functions at two MODIS bands centered at 0.65 μm (or 0.86 μm) and 2.13 μm are investigated. The Level-3 MODIS ice cloud properties (specifically, ice cloud fraction, optical thickness, and effective particle size in this study) from the Collection 4 and 5 datasets are compared for a tropical belt of 30°S–30°N. Furthermore, the impact of the differences between the MODIS Collection 4 and 5 ice cloud products on the simulation of the radiative forcing of these clouds is investigated. Over the tropics, the averaged ice cloud fraction from Collection 5 is 1.1% more than the Collection 4 counterpart, the averaged optical thickness from Collection 5 is 1.2 larger than the Collection 4 statistics, and the averaged effective particle radius from Collection 5 is 1.8 μm smaller than the Collection 4 result. Moreover, the magnitude of the differences between the Collection 5 and 4 ice cloud properties also depend on the surface characteristics, i.e., over land or over ocean. The differences of these two datasets (Collections 5 and 4) of cloud properties can have a significant impact on the simulation of the radiative forcing of ice clouds. In terms of total (longwave plus shortwave) cloud radiative forcing, the differences between the Collection 5 and 4 results are distributed primarily between -60 Wm^{-2} and 20 Wm^{-2}, peaked at 0 Wm^{-2}.

Index Terms—MODIS, Aqua, clouds, lookup libraries, remote sensing, radiative forcing.

I. Introduction

With the increasing awareness of the importance of ice clouds [25], [29] in the terrestrial atmosphere, research has addressed numerous issues relevant to ice clouds from various perspectives, including *in situ* measurements of the microphysical properties of ice clouds [13], theoretical investigations of the single and multiple scattering and absorption properties of ice clouds [1], [30], [36], [37], [47], [48], [55], [56], [59] efforts to parameterize the bulk radiative properties of these clouds [7], [8], [10], [33] for applications to climate models, the impacts of ice clouds on the radiation spectrum [52] and climate feedback [45], and the retrieval of ice cloud optical and microphysical properties from airborne and satellite measurements [1], [2], [6], [15], [20], [22], [34], [35], [51]. However, the representation of these clouds in general circulation models (GCMs) is rather primitive in the sense that substantial uncertainties exist in the basic cloud climatologies derived from the GCM simulations, and the cloud distributions simulated from many GCMs are quite different from those inferred from satellite observations [60]. To improve the representation of ice clouds in GCMs, it is critical to understand the global ice cloud climatology to provide crucial constraints on the parameterization of various cloud microphysical processes and cloud-radiation interactions in GCMs. To this end, reliable satellite-based retrievals of ice cloud properties on a global scale are necessary.

The Moderate Resolution Imaging Spectroradiometer (MODIS) instruments [17], [18], [54] on the NASA Earth Observation (EOS) Terra and Aqua platforms include 36 spectral channels covering essentially all the key atmospheric bands located between 0.415 μm and 14.235 μm [41] and provide advanced capabilities to study ice clouds, although MODIS does not have far-infrared-radiation (far-IR) spectral bands. The far-IR is important to the energetics of the earth's atmosphere. The MODIS measurements have been extensively used in cloud property retrievals or cloud-clearing (e.g., [23], [24]). With pre-computed lookup libraries of ice cloud radiances, a bispectral technique [39] can be used to simultaneously infer the optical thickness and effective particle size of an

ice cloud from the MODIS measurements [18], [21], [41] during daytime conditions. The MODIS cloud (Level-2) pixel-level products are available for individual granules, known as MOD06 and MYD06 for Terra and Aqua, respectively (note that the product prefix "MOD" is used for the retrieval products based on the measurements acquired from the Terra platform whereas "MYD" is used for the retrieval products based on the measurements acquired from the Aqua platform), and also as global (Level-3) 1°x1° gridded datasets.

Recently, substantial improvements have been made on the MODIS cloud products and new datasets (Collection 5) are available [19]. In this study, we first illustrate the effect of the differences of the bulk optical properties of ice particles on the simulation of the bidirectional reflection function for ice clouds that are essential to the MODIS operational retrieval. Then, we compare the operational MODIS Collections 4 and 5 ice cloud properties. Specifically, the analysis presented in this article focuses on the MODIS Level-3 ice cloud fraction, ice cloud optical thickness and effective particle size, although a case study involving the MODIS Level-2 data is also presented. Furthermore, we investigate the potential impacts of the MODIS Collection 5 improvements on the simulation of the radiative forcing of ice clouds.

II. Lookup Libraries for Retrieving Ice Cloud Properties

King *et al.* [18] provide an overview of the data architecture and products of the MODIS operational atmospheric parameter data products. In summary, the MOD06 and MYD06 datasets contain the pixel-level (or the so-called Level-2) retrievals performed for individual granules, i.e., datasets corresponding to 5-minute scans of the MODIS instruments along their orbit tracks. The Level-2 products are further mapped onto Level-3 products (MOD08 and MYD08) with a spatial resolution of 1°x1° in latitude and longitude on a daily, eight-day and monthly mean basis.

Platnick *et al.* [41] discuss the pixel-level retrieval of the optical and microphysical properties (i.e., optical thickness and effective particle size) on the basis of the bispectral method developed by Nakajima and King [39]. The physical basis of this retrieval method is that the radiance observed by a satellite sensor at a non-absorbing band (e.g., a band centered at a wavelength of 0.65 μm) under cloudy conditions is sensitive primarily to cloud optical thickness and insensitive to the effective particle sizes, whereas the radiances observed at an absorbing band (e.g., a band centered at a wavelength of 2.13 μm) under cloudy conditions are sensitive to the effective particle size. Thus, a pair of the radiances measured at these two bands in comparison with theoretical radiance correlation (i.e., the so-called lookup tables that are pre-computed for the implementation of the retrieval algorithm) between the two bands allows simultaneous retrieval of cloud optical thickness and effective particle size. For the operational MOD06 retrieval algorithm [41], the MODIS 0.65 μm band (for over land), 0.86 μm (for over ocean), or 1.24 μm band (for over ice/snow surfaces) is used as a non-absorbing band involved in the bispectral retrieval algorithm. The availability of the three bands for various surface characteristics helps to mitigate the influence of the surface reflectance [41] on the retrievals. The operational retrieval algorithm uses the 2.13 μm band as an absorbing band for implementing the bispectral algorithm. Additionally, retrievals based on the 1.64 or 3.78 μm band in combination for a non-absorbing band (e.g., 0.65, 0.84, or 1.24 μm band) provide information about the deviations from those retrieved on the basis of a combination of the 2.13 μm band with a nonabsorbing band (e.g., the 0.65 μm band), as explained by Platnick *et al.* [41]. According to the physical basis of the aforementioned bispectral cloud retrieval algorithm, the theoretical correlation of the lookup tables of the reflection functions at the absorbing and non-absorbing bands is fundamental to the operational MODIS cloud retrieval.

Recently, the MODIS atmosphere team has implemented and delivered an update (known as Collection 5) for the operational cloud products. As summarized by King *et al.*

[19], the lookup libraries of the bidirectional reflectances, transmittances, and spherical albedos of ice clouds (i.e., the so-called ice libraries) at absorbing and non-absorbing bands involved in the MODIS bispectral retrieval algorithm have been improved. Additionally, several major improvements have also been made on the MODIS cloud retrievals. The new ice libraries improve the MODIS operational retrievals of ice cloud optical and microphysical properties (i.e., optical thickness and effective particle size). To generate the ice libraries, the fundamental single-scattering properties (i.e., phase function, single-scattering albedo, and mean volume extinction coefficient) of ice particles are required. A major difference between the Collection 4 and 5 ice cloud properties stems from different treatments of small ice crystals. In the light scattering computations for the MODIS Collection 4 ice cloud products, small ice particles are assumed to be compact hexagonal ice particles with a unit aspect ratio (i.e., $L/a = 2$ where L and a are the length and semiwidth of an ice particle, respectively), whereas a droxtal geometry [40], [49], [56], [61] is assumed to approximately represent the habits (or shapes) of small quasi-spherical ice particles in the MODIS Collection 5 ice cloud retrievals.

To generate the bulk single-scattering properties of ice particles for the forward radiative transfer simulations required for the development of the lookup libraries, it is necessary to account for the effect of the assumed particle size and habit distribution. For the MODIS Collection 4, twelve size distributions acquired for midlatitude ice cloud systems were used, which were discretized into 5 size bins with a coarse resolution. For a given size distribution, the percentage of ice particle habits is assumed as follows [3], [20]: 25% plates, 25% hollow columns, and 50% bullet rosettes for size bins (in particle maximum dimension) smaller than 70 μm; and 20% plates, 20% hollow columns, 30% bullet rosettes, and 30% aggregates for size bins larger than 70 μm. The surface of aggregates is slightly roughened. For the MODIS Collection 5 ice cloud products, 1117 size distributions acquired for tropical, subtropical and midlatitude ice cloud systems [4], [5] are used. These size distributions are discretized into 45 size bins with a cutoff of 9500 μm. The

habit percentage was determined by fitting the *in situ* ice water content and median mass diameter [4], given by 100% droxtals for size bins less than 60 μm; 35% plates, 15% bullet rosettes, 50% solid columns, for size bins between 60 μm and 1000 μm; 45% solid columns, 45% hollow columns, 10% aggregates for size bins between 1000 μm and 2000 μm; and 3% aggregates and 97% bullet rosettes for size bins larger than 2000 μm. The bulk single-scattering properties computed are integrated over size distributions and habit mixture reported in Baum *et al.* [4], [5].

Figure 1 shows the comparison of the phase functions used for the MODIS Collection 4 and 5 ice cloud retrievals at two wavelengths, 0.65 μm and 2.13 μm for a small and moderate effective particle size. Note that for Collection 4, the minimum effective particle radius is 6.7 μm whereas it is 5 μm for the MODIS Collection 5. For small sizes, the Collection 4 phase function has larger values, relative to its Collection 5 counterpart, at the side scattering angles (50°-110°) because the droxtal geometry is used for small particles in the Collection 5 scattering computations. However, the Collection 4 phase function is smaller in the backscattering angles (120°-180°). This occurs because hollow columns (with a percentage of 25% when the particle maximum dimension is less than 70 μm) are assumed for computing the Collection 4 phase functions. Hollow columns scatter much less energy in backscattering directions than solid columns [48], [57]. Especially, there are major differences between the phase functions of Collections 4 and 5 for small effective radii at the scattering angles between 40º and 180º. For a moderate effective radius (20 μm), the two versions of phase functions are quite similar although some differences are noticed, particularly at scattering angles between 10°-20° and 120°-180°. Based on the phase function differences in Fig.1, differences are expected between the satellite retrieved effective particle size and optical thickness datasets from the MODIS Collection 4 and 5, particularly in the case of ice clouds with small particles.

The effective particle size (radius) in Fig. 1 and also that used in the MODIS operational cloud retrieval is defined as follows ([3], [4], [20] and references cited therein):

$$r_e = \frac{3}{4}\frac{\sum_i \int V_i(D)n(D)f_i(D)dD}{\sum_i \int A_i(D)n(D)f_i(D)dD}, \quad (1)$$

where V, A, and D are the geometric volume, orientation-averaged projected area, and maximum dimension of an ice particle, respectively. The quantity, $n(D)$, denotes the size distribution as a function of ice particle maximum dimension. The parameter f_i indicates the percentage of each ice particle habit (shape). As noted by King *et al.* [20], the definition given in Eq. (1) reduces to that given by Hansen and Travis [11] in the case of spherical particles. Another advantage of the definition specified by Eq. (1) for the effective particle size is that the ice water path (IWP) of an ice cloud can be given by [9], [26], [27], [31]

$$IWP = \frac{4}{3}\frac{\rho_e \tau r_e}{< Q_e >} \approx \frac{2}{3}\rho_e \tau r_e, \quad (2)$$

where τ is the visible optical thickness of an ice cloud, ρ_e (~0.917 gcm^{-3}) is the density of bulk ice, and $< Q_e >$ is the mean extinction efficiency for a population of ice particles, as described by [58]

$$< Q_e >= \frac{\sum_i \int Q_{e,i}(D)A_i(D)f_i(D)n(D)dD}{\sum_i \int A_i(D)f_i(D)n(D)dD}. \quad (3)$$

In Eq. (2), it is assumed that $< Q_e >$ is approximately 2. This is an accurate approximation because the sizes of ice particles are normally much larger than the visible or near-infrared wavelengths, and consequently, the extinction cross sections of these particles are twice their projected areas [50]. It is evident from Eq. (2) that the MODIS cloud products implicitly provide information about ice water path, as it can be derived from the retrieved optical thickness and effective particle size in a straightforward manner.

Figure 2 shows the comparison of the correlation between the bidirectional reflection functions for the MODIS 0.65- and 2.13-μm bands computed from the Collection 4

and 5 bulk single-scattering properties. In the present radiative transfer computations, the solar zenith angle (θ_0) and satellite-viewing angle (θ) are 30° and 0°, respectively. Over land and ocean, the surface albedo is assumed to be 0.2 and 0.03, [38], [41] respectively. The radiative transfer simulations in Fig. 2 are based on the Discrete Ordinates Radiative Transfer (DISORT) model developed by Stamnes *et al.* [44]. The gaseous absorption is neglected in the present simulations. It is evident from Fig. 2 that the range of effective particle sizes covered in Collection 5 is larger than that for Collection 4. Furthermore, substantial differences are noted in terms of the isolines of effective particle size. For example, in both land and ocean cases, the isoline of r_e = 25 μm computed from the Collection 5 ice cloud optical properties is much lower than the Collection 4 counterpart, and follows the Collection 4 28-μm isoline. This implies that retrieved effective particle sizes in Collection 5 might be smaller than those in Collection 4. In terms of the isolines of optical thickness shown in Fig.2, the results for Collection 5 and 4 are similar, but some differences are noticed for small and large particles (i.e., r_e < 10 μm and r_e > 25 μm). From a detailed scrutiny of the differences in the correlation of the reflection functions shown in Fig. 2, it is noticed that the retrieved optical thickness in Collection 5 will deviate from those in Collection 4 on the order of $\Delta\tau \sim 2$.

For operational cloud retrievals, it is impractical to carry out forward radiative transfer computations for individual pixels and various sun-satellite geometries by using a rigorous radiative transfer model (e.g., DISORT). Instead, lookup libraries of the reflection and transmission functions of clouds with various optical thicknesses and effective particle sizes must be used. For the MODIS operational cloud retrieval algorithm, the static libraries of the bidirectional reflectance, total transmittance, and spherical albedo of clouds are generated by assuming a blackbody underlying surface without consideration of the absorption by atmospheric gases [41]. The effect of surface albedo is taken into account on the basis of the adding/doubling principle in a way explained in King *et al.* [21] as follows:

$$R(\mu,\mu_0,\Delta\varphi) = R_{cloud}(\mu,\mu_0,\Delta\varphi) + \frac{T(\mu_o)r_g T(\mu)}{1 - r_g \overline{R}_{cloud}}, \quad (4)$$

where μ, μ_0, and Δϕ indicate the cosine of view zenith angle, the cosine of the solar zenith angle, and relative azimuthal angle between the sun and the satellite, respectively. The quantity r_g indicates the surface albedo. R is the apparent reflectance observed by the satellite. R_{cloud}, T, and $\overline{R}_{cloud}$ are the cloud bidirectional reflectance, total transmittance, and spherical albedo, respectively, which are functions of the optical thickness and effective particle size of the cloud of interest. The preceding formula provides a computationally efficient way to compute the theoretical radiances with which the measured radiances are compared in the retrieval process. In practice, R_{cloud}, T, and $\overline{R}_{cloud}$ are pre-computed, representing the so-called ice libraries for implementing an operational bispectral cloud retrieval algorithm. Evidently, the reliability of the ice libraries is critical to the accuracy of retrieved optical thickness and effective particle size.

III. Comparison between MODIS Collection 4 and 5 Ice Cloud Properties

To compare the Collection 4 and 5 Level-2 ice cloud products, we select a granule acquired on July 1, 2004, over Southeast Asia. Figure 3 shows the comparison of the optical thickness and effective particle size from the MYD06 product for this granule. The cloud phase flag in the MYD06 Quality Assurance (QA) is used to screen out those pixels that are identified as not being associated with ice clouds. It is evident from Fig. 3 that Collection 5 data, overall, show larger optical thicknesses and smaller ice particle effective sizes than Collection 4, though in some instances clouds identified as ice in Collection 4 are identified as liquid water in Collection 5.

The present comparison of the MODIS Collection 5 and 4 ice cloud properties is intended to focus on the Level-3 products because they are more manageable than the Level-2 data from a climate modeler's perspective. Specifically, we select Collection 4 and 5 Level-3 ice cloud products from MYD08_D3 over the tropics (between 30S and 30N) from January 2004 to December 2004. The simple statistics of mean or QA-

weighted mean for high cloud properties with each grid box are available in the MYD08_D3 products [18]. Cloud fraction can be derived as the ratio of the total counts flagged with clouds to the total number of observed pixels within a given grid box. The high-level cloud optical thickness and effective particle size inferred from the MODIS visible and near-infrared channel radiances are directly taken from the QA-weighted means in the MYD08_D3 products.

Figure 4 shows the geographical distributions of high cloud fraction, optical thickness, and effective radius over the tropics (30°S–30°N) from Aqua MODIS Collection 4 and 5. The overall features of the distribution of ice clouds are consistent with those reported in the literature [14], [42], [43], [46], [53]. Ice clouds occur frequently over the Intertropical Converge Zone (ITCZ), the South Pacific Converge Zone (SPCZ), tropical Africa, tropical America, Indonesia maritime continent, and Indian Ocean. The ice cloud fractions from Collection 5 increase over land and decrease over ocean with respect to those from Collection 4. The ice cloud optical thicknesses and ice particle effective sizes from Collection 5 show the same geographical features as those from Collection 4. The land-ocean contrast is also found for ice cloud optical thicknesses. The cloud optical thicknesses from Collection 5 are apparently larger over ocean and smaller over land than those from Collection 4. The ice cloud particle effective sizes from Collection 5 are generally smaller than those from Collection 4. Over Northern Africa, the cloud effective particle sizes from Collection 5 have significantly larger values than those from Collection 4.

Figure 5 shows the histogram distributions of ice cloud fraction, optical thickness, and effective particle radius over ocean and land. Statistically, ice cloud fraction over land from the Collection 5 data set have larger values in comparison with its Collection 4 counterparts, whereas the two data sets are only slightly different in the case of ice clouds over ocean. Ice cloud optical thicknesses from Collection 5 over land have a frequency distribution similar to that from Collection 4. The distributions of ice particle effective

sizes from Collection 5 over both land and ocean are shifted to smaller values in comparison with the Collection 4 results.

Table 1 lists the one-year mean results of ice cloud fraction, optical thickness, and effective particle size, and ice water path (IWP) from the Collection 5 and 4 data over the tropics (30°S–30°N) from January 2004 to December 2004. The IWP values are estimated from the corresponding optical thickness and effective particle size on the basis of Eq. (2). Note that the mass density of bulk ice is assumed to be 0.917 gcm^{-3} in this study. The mean ice cloud fraction of Collection 5 is 25.1%, which is 1.1% larger than that of the Collection 4 result. Ice cloud fraction from Collection 5 increases 6.1% over land but decreases 0.8% over ocean, indicating that the land-ocean contrast in Collection 5 is stronger than that in the case of Collection 4. Cloud optical thickness decreases 0.3 over land and increases 1.9 over ocean for Collection 5 in comparison with their Collection 4 counterparts. This results in an increase of 1.2 in the mean value of cloud optical thickness. The optical thicknesses in Collection 5 show a weak land-ocean contrast whereas those in Collection 4 have a significant contrast. The *IWP* values estimated from the Collection 5 data, averaged over the tropics, are larger over ocean and smaller over land than the corresponding Collection 4 estimates. Specifically, the values of $(IWP_5 - IWP_4)/IWP_4$ are –9.7%, 9.5%, and 2.2% for land, ocean, and total statistics, respectively.

The ice cloud radiative forcing based on Collection 4 and 5 is shown in Figure 6. The ice cloud radiative forcing is calculated with the radiative transfer code LibRadtran [32]. A new scheme (J. Lee, personal communication) of parameterizing the bulk optical properties of ice clouds, which is based on the database of the single-scattering properties of individual ice particles developed by Yang *et al.* [57], [59], is used in the present cloud radiative forcing simulation. The ice cloud optical thickness, effective particle size, and cloud top height from MYD_08 products are used for LibRadtran. Following Hong *et al.* [14], we use the ISCCP classification [42], [43] to identify ice clouds (cloud top pressure less than 440 hPa) using the MYD_08 daily products, and then average the daily ice

cloud properties over a period from January 2004 to December 2004. The standard atmospheric profile in the tropics is used as the input for atmospheric condition in LibRadtran. Following Liou and Gebhart [28], in this study the solar zenith angle is assumed to be 60° to represent an approximate average for a solar day with a 12-hour duration of sunlight.

The net shortwave (solar) and longwave (infrared) fluxes at the top of the atmosphere (TOA) are defined as follows:

$$F_{sw} = F_{sw}^{\downarrow} - F_{sw}^{\uparrow}, \tag{5}$$

$$F_{lw} = -F_{lw}^{\uparrow}, \tag{6}$$

where the symbols ↑ and ↓ indicate upward and downward radiation, respectively. $F_{lw}^{\uparrow}$ is also known as the outgoing longwave radiation (OLR), a term often used in the literature (e.g., [26]). For a partially cloudy region with a cloud fraction of *N*, the average-sky net TOA flux is given by [26]

$$F = N(F_{sw,cloud} + F_{lw,cloud}) + (1-N)(F_{sw,clear} + F_{lw,clear}). \tag{7}$$

Following Hartmann *et al.* [12], the cloud radiative forcing (CRF) is given by

$$CRF = F - F_{clear}. \tag{8}$$

Note that the sign on the right-hand side of Eq. (8) is different from the expression given by Liou [26] (p. 379). CRF can be further decomposed into the shortwave and longwave components as follows:

$$CRF = CRF_{sw} + CRF_{lw}, \tag{9}$$

where

$$CRF_{sw} = N(F_{sw,cloud} - F_{sw,clear}), \tag{10}$$

$$CRF_{lw} = N(F_{lw,cloud} - F_{lw,clear}). \tag{11}$$

From Fig. 6, the shortwave radiative forcing of ice clouds is negative, indicating the cooling effect of ice clouds, while the longwave radiative forcing of ice clouds is posi-

tive, indicating the warming effect of ice clouds. The net radiative effect of ice particles depends strongly on the competition of the heating and warming effects, which is most sensitive to the optical thicknesses of ice clouds [16]. The shortwave radiative forcing is much stronger than the longwave radiative forcing for higher optical thicknesses. This results in the total radiative forcing being negative in sign. The shortwave, longwave, and total radiative forcing of ice clouds in Collection 5 have similar geographical distributions as those in Collection 4. The pronounced radiative forcing appears over land. In general, the negative shortwave, positive longwave, and negative total radiative forcing in Collection 5 are stronger over land and weaker over ocean than those in Collection 4. Differences in CRF between Collection 4 and 5 tend to be larger over land.

Fig. 7 shows the Collection 5 cloud radiative forcing versus its Collection 4 counterpart, and a one-to-one line is also shown. For shortwave radiation, the Collection 5 results are close to the Collection 4 results although some smaller values for the former are noticed. For longwave radiation, the Collection 4 and 5 results are also similar, but some larger values for the Collection 5 results are observed. In terms of the total radiative forcing of ice clouds, the Collection 5 results have smaller values. The right three panels in Fig. 7 show the histograms of the frequency distributions of the differences between the Collections 4 and 5 cloud radiative forcing. The differences between the Collections 5 and 4 CRF peak around 0 Wm^{-2} for shortwave, longwave, and total radiation, respectively. The differences between the Collection 5 and 4 total radiative forcing distribute between -60 Wm^{-2} and 20 Wm^{-2}.

Plotted in Figures 8 and 9 are the radiative forcings of ice clouds as a function of cloud optical thickness and effective particle size, respectively. The results in Fig. 8 indicate that the cloud radiative forcing increases in magnitude with the increase of cloud optical thickness. However, a monotonic relationship between CRF and cloud optical thickness cannot be obtained from the results shown in Fig. 8.

The results shown in Fig. 9 indicate that the distribution of particle effective sizes peaks between 20 and 30 μm. A monotonic relationship between CRF and effective particle size cannot be derived from the results shown in Fig. 9.

IV. SUMMARY

In this article we first compare the differences of the bulk optical properties of ice clouds used in the MODIS Collection 4 and 5 ice cloud retrievals. We investigate the effect of these differences on the forward radiative transfer simulations required for generating the static libraries of the ice cloud bidirectional reflection functions over a range of optical thicknesses and effective particle sizes. Our study indicates that the theoretical relationship between the reflection functions at two bands (e.g., 0.65 μm and 2.13 μm) computed from the ice cloud optical models for Collection 5 may lead to smaller effective particle sizes in comparison with their Collection 4 counterparts. The effect on the retrieval of optical thickness is noticed primarily for the smallest and largest effective particle sizes.

One-year (January 2004-December 2004) data of Aqua/MODIS ice cloud fraction, effective particle size, and optical thickness from both Collection 4 and 5 are compared for the tropical belt (30°S-30°N). On average, the Collection 5 ice cloud fraction is 6.1% larger and 0.8% smaller than the Collection 5 data over land and ocean, respectively. In terms of optical thickness, the Collection 5 results are 0.3 smaller and 1.9 larger than their Collection 4 counterparts over land and ocean, respectively. In terms of effective particle size, the Collection 5 results are 1.9 μm and 1.7 μm smaller than the Collection 4 counterparts over land and ocean, respectively.

Furthermore, we investigate the impact of the differences between Collection 4 and 5 ice cloud products to assess the radiative forcing of these clouds. The differences in the total cloud forcing are primarily between -60 Wm^{-2} and 20 Wm^{-2} and peak at 0 Wm^{-2}. Thus, the differences between Collection 4 and 5 ice cloud products can lead to either an

enhancement or a reduction of the warming effect of ice clouds, depending on a specific ice cloud of interest. From the radiative forcing perspective, the differences found between Collection 4 and 5 ice cloud products demonstrate the need to correctly characterize the scattering and absorption properties if climate models are to be further improved.

ACKNOWLEDGEMENT

This effort is supported by a NASA research grant (NNG04GL24G) from NASA Radiation Sciences Program managed by Dr. Hal Maring (previously by Dr. Donald Anderson) and the MODIS Program managed by Dr. Paula Bontempi. Regarding the development of the radiative properties (the single-scattering properties, in particular) of ice clouds from theoretical perspective, Ping Yang also acknowledges support from the National Science Foundation Physical Meteorology Program (ATM-0239605) managed by Dr. Andrew Detwiler.

REFERENCES

[1] A. J. Baran, P. N. Francis, S. Havemann, and P. Yang, "A study of the absorption and extinction properties of hexagonal ice columns and plates in random and preferred orientation, using exact T-matrix theory and aircraft observations of cirrus," *J. Quant. Spectrosc. Radiat. Transfer*, vol. 70, pp. 505-518, 2001.

[2] A. J. Baran, P. N. Francis, L. C. Labonnote and M. Doutriaux-Boucher, "A scattering phase function for ice cloud tests of applicability using aircraft and satellite multi-angle multi-wavelength radiance measurements of cirrus," *Quart. J. Roy. Meteorol. Soc.,* vol. 127, pp. 2395-2416, 2001.

[3] B. A. Baum, D. P. Kratz, P. Yang, S.C. Ou, Y. Hu, P. Soulen, and S. C. Tsay, "Remote sensing of cloud properties using MODIS airborne simulator imagery during SUCCESS. I. Data and Models," *J. Geophys. Res.,* vol. 105, pp. 11767-11780, 2000.

[4] B. A. Baum, A. J. Heymsfield, P. Yang, and S. T. Bedka, "Bulk scattering properties for the remote sensing of ice clouds. Part I: Microphysical data and models," *J. Appl. Meteor.,* vol. 44, pp. 1885-1895, 2005.

[5] B. A. Baum, P. Yang, A. J. Heymsfield, S. Platnick, M. D. King, Y. X. Hu, and S. T. Bedka, "Bulk scattering properties for the remote sensing of ice clouds. Part II: Narrowband models," *J. Appl. Meteor.,* vol. 44, pp. 1896-1911, 2005.

[6] H. Chepfer, P. Minnis, D. F. Young, L. Nguyen, and R. F. Arduini, "Estimation of cirrus cloud effective ice crystal shapes using visible reflectances from dual-satellite measurements," *J. Geophys. Res.,* vol. 107, 10.1029/2000JD000240, 2002.

[7] E. E. Ebert, and J. A. Curry, "A parameterization of ice cloud optical properties for climate models," *J. Geophys. Res.*, vol. 97, pp. 3831-3836, 1992.

[8] J. M. Edwards, S. Havemann, J. C. Thelen, and A. J. Baran, "A new parameterization for the radiative properties of ice crystals: Comparison with existing schemes

and impact in a GCM," *Atmos. Res*., vol. 83, pp. 19-35, 2007.

[9] P. N. Francis, A. Jones, R. W. Saunders, K. P. Shine, A. Slingo, and Z. Sun, "An observational and theoretical study of the radiative properties of cirrus: Some results from ICE'89," *Quart. J. Roy. Meteor. Soc.,* vol. 120**,** pp. 809-848, 1994.

[10] Q. Fu, P. Yang, and W. B. Sun, "An accurate parameterization of the infrared radiative properties of cirrus clouds for climate models," *J. Climate*., vol. 25, pp. 2223-2237, 1998.

[11] J. E. Hansen, and L. B. Travis, "Light scattering in planetary atmospheres," *Space. Sci. Rev.,* vol. 16, pp. 527-610, 1974.

[12] D. L. Hartmann, L. A. Moy, and Q. Fu, "Tropical convection and energy balance at the top of the atmosphere," *J. Climate,* vol. 14, pp. 4495-4511, 2001.

[13] A. J. Heymsfield, A. Bansemer, P. Field, S. L. Durden, J. Stith, J. E. Dye, W. Hall, and T. Grainger, "Observations and parameterizations of particle size distributions in deep tropical cirrus and stratiform precipitating clouds: Results from in situ observations in TRMM field campaigns," *J. Atmos. Sci*., vol. 59, pp. 3457-3491, 2002.

[14] G. Hong, P. Yang, B. C. Gao, B. A. Baum, Y. X. Hu, M. D. King, and S. Platnick, "High cloud properties from three years of MODIS Terra and Aqua Collection 4 Data over the Tropics," *J. Appl. Meteor. Climatol.,* in press, 2007.

[15] H. L. Huang, P. Yang, H. Wei, B.A. Baum, Y. X. Hu, P. Antonelli, and S. A. Ackerman, "Inference of ice cloud properties from high-spectral resolution infrared observations," *IEEE Trans. Geosci. Remote Sens,* vol. 42, pp. 842-852, 2004.

[16] E. J. Jensen, K. Kinne, and O. B. Toon, "Tropical cirrus cloud radiative forcing: sensitivity studies," *Geophys. Res. Lett.*, vol. 12, pp. 2023-2026, 1994.

[17] M. D. King, Y. J. Kaufman, W. P. Menzel, and D. Tanré, "Remote sensing of cloud, aerosol, and water vapor properties from the Moderate Resolution Imaging Spectrometer (MODIS)," *IEEE Trans. Geosci. Remote Sens.*, vol. 30, pp. 2-27, 1992.

[18] M. D. King, W. P. Menzel, Y. J. Kaufman, D. Tanré, B. C. Gao, S. Platnick, S. A. Ackerman, L. A. Remer, R. Pincus, and P. A. Hubanks, "Cloud and aerosol properties, precipitable water, and profiles of temperature and humidity from MODIS," *IEEE Trans. Geosci. Remote Sens.*, vol. 41, pp. 442-458, 2003.

[19] M. D. King, S. Platnick, P. A. Hubanks, G. T. Arnold, E. G. Moody, G. Wind, and B. Wind, "Collection 005 change summary for the MODIS cloud optical property (06_OD) algorithm," (available at modis-atmos.gsfc.nasa.gov/C005_Changes/C005_CloudOpticalProperties_ver311.pdf), 2006.

[20] M. D. King, S. Platnick, P. Yang, G. T. Arnold, M. A. Gray, J. C. Riédi, S. A. Ackerman, and K. N. Liou, "Remote sensing of liquid water and ice cloud optical thickness, and effective radius in the arctic: Application of air-borne multispectral MAS data," *J. Atmos. and Ocean. Technol.*, vol. 21, pp. 857-875, 2004.

[21] M. D. King, S. C. Tsay, S. E. Platnick, M. Wang, and K. N. Liou, "Cloud retrieval algorithms for MODIS: Optical thickness, effective particle radius, and thermodynamic phase," MODIS Algorithm Theoretical Basis Document No. ATBD-MOD-05, 79 pp. (available at modis-atmos.gsfc.nasa.gov/_docs/atbd_mod05.pdf), 1997.

[22] A. A. Kokhanovsky, and T. Nauss, "Satellite based retrieval of ice cloud properties using semianalytical algorithm," *J. Geophys. Res.*, vol. D110, D19206, doi: 10.1029/2004JD005744, 2005.

[23] A. A. Kokhanovsky, T. Nauss, M. Schreier, W. von Hoyningen-Huene, and J. P. Burrows, "The intercomparison of cloud parameters derived using multiple satellite instruments," *IEEE Trans. Geosci. Remote Sens*., vol. 45, pp. 195-200, 2007.

[24] J. Li, C. Y. Liu, H. L. Huang, T. J. Schmit, X. Wu, W. P. Menzel, and J. J. Gurka, "Optimal cloud-clearing for AIRS radiances using MODIS," *IEEE Trans. Geosci. Remote Sens.*, vol. 43, pp. 1266-1278, 2005.

[25] K. N. Liou, "Influence of cirrus clouds on weather and climate process: A global

perspective," *Mon. Weather Rev.*, vol. 114, pp. 1167-1199, 1986.

[26] K. N. Liou, *Radiation and Cloud Processes in the Atmosphere—Theory, Observation, and Modeling*. New York: Oxford University Press, 1992.

[27] K. N. Liou, *An Introduction to Atmospheric Radiation*, San Diego, CA: Academic Press, 2002.

[28] K. N. Liou, and K. L. Gebhart, "Numerical experiments on the thermal equilibrium temperature in cirrus cloudy atmospheres," *J. Meteor. Soc. Japan,* vol. 60, pp. 570-582, 1982.

[29] D. K. Lynch, K. Sassen, D. OC Starr, and G. Stephens (eds.), *Cirrus*, New York: Oxford University Press, 2002.

[30] A. Macke, J. Mueller, and E. Raschke, "Single scattering properties of atmospheric ice crystal," *J. Atmos. Sci.,* vol. 53, pp. 2813-2825, 1996.

[31] A. Mahesh, V. P. Walden, and S. G. Warren, "Ground-based infrared remote sensing of cloud properties over the Antarctic Plateau, Part II: Cloud optical depths and particle sizes," *J. Appl. Meteor.,* vol. 40, pp. 1279-1294, 2001.

[32] B. Mayer and A. Kylling, "Technical Note: The libRadtran software package for radiative transfer calculations: Description and examples of use," *Atmos. Chem. Phys.,* vol. 5, pp. 1855-1877, 2005.

[33] G. M. McFarquhar, P. Yang, A. Macke, and A. J. Baran, "A new parameterization of single-scattering solar radiative properties for tropical anvils using observed ice crystal size and shape distributions," *J. Atmos. Sci.*, vol. 59, pp. 2458-2478, 2002.

[34] P. Minnis, P. W. Heck, and D. F. Young, "Inference of cirrus cloud properties using satellite-observed visible and infrared radiances, Part II: Verification of theoretical cirrus radiative properties," *J. Atmos. Sci.*, vol. 50, pp. 1305-1322, 1993.

[35] P. Minnis, Y. Takano, and K. N. Liou, "Inference of cirrus cloud properties using satellite-observed visible and infrared radiances, Part I: Parameterization of radiance fields," *J. Atmos. Sci.*, vol. 50, pp. 1279-1304, 1993.

[36] M. I. Mishchenko, W. B. Rossow, A. Macke, and A. A. Lacis, "Sensitivity of cirrus cloud albedo, bidirectional reflectance and optical thickness retrieval accuracy to ice particle shape," *J. Geophys. Res.,* vol. 101, pp. 16973-16985, 1996.

[37] D. L. Mitchell, A. J. Baran, W. P. Arnott, and C. Schmitt, "Testing and comparing the modified anomalous diffraction approximation," *J. Atmos. Sci*., vol. 63, pp. 2948-2962, 2001.

[38] E. G. Moody, M. D. King, S. Platnick, C. B. Schaaf, and F. Gao, "Spatially complete global spectral surface albedos: value-added datasets derived from Terra MODIS land products," *IEEE Trans. Geosci. Remote Sens.*, vol. 43, pp. 144-158, 2005.

[39] T. Nakajima, and M. D. King, "Determination of the optical thickness and effective particle radius of clouds from reflected solar radiation measurements. Part I: Theory," *J. Atmos. Sci.,* vol. 47, pp. 1878-1893, 1990.

[40] T. Ohtake, "Unusual crystal in ice fog," *J. Atmos. Sci.,* vol. 27, pp. 509-511, 1970.

[41] S. Platnick, M. D. King, S. A. Ackerman, W. P. Menzel, B. A. Baum, J. C. Riédi, and R. A. Frey, "The MODIS cloud products: Algorithms and examples from Terra," *IEEE Trans. Geosci. Remote Sens.*, vol. 41, pp. 459-473, 2003.

[42] W. B. Rossow, and R. A. Schiffer, "ISCCP cloud data products," *Bull. Amer. Meteor. Soc.,* vol. 72, pp. 2–20, 1991.

[43] W. B. Rossow, and R. A. Schiffer, "Advances in understanding clouds from ISCCP," *Bull. Amer. Meteor. Soc.,* vol. 80, pp. 2261–2287, 1999.

[44] K. Stamnes, S. C. Tsay, W. Wiscombe, and K. Jayaweera, "A numerically stable algorithm for discrete-ordinate-method radiative transfer in multiple scattering and emitting layered media," *Appl. Opt.,* vol. 27, pp. 2502-2509, 1988.

[45] G. L. Stephens, S. C. Tsay, P. W. Stackhouse, and P. J. Flatau, "The relevance of the microphysical and radiative properties of cirrus clouds to climate and climate feedback," *J. Atmos. Sci.,* vol. 47, pp. 1742-1753, 1990.

[46] C. J. Stubenrauch, A. Chédin, G. Rädel, N. A. Scott, and S. Serrar, "Cloud proper-

ties and their seasonal and diurnal variability from TOVS," *submitted to J. Climate,* 2006.

[47] Y. Takano, and K. N. Liou, "Solar radiative transfer in cirrus clouds. Part I. Single-scattering and optical properties of hexagonal ice crystals," *J. Atmos. Sci.,* vol. 46, pp. 3-19, 1989.

[48] Y. Takano, and K. N. Liou, "Radiative transfer in cirrus clouds. Part III: Light scattering by irregular ice crystals," *J. Atmos. Sci.,* vol. 52, pp. 818-837, 1995.

[49] W. C. Thuman, and E. Robinson, "Studies of Alaskan ice-fog particles," *J. Meteor.,* vol. 11, pp. 151-156, 1954.

[50] H. C. van de Hulst, *Light Scattering by Small Particles*, Wiley, New York, 470 pp., 1957.

[51] H. Wei, P. Yang, J. Li, B. A. Baum, H. L. Huang, S. Platnick, Y. X. Hu, and L. Strow, "Retrieval of ice cloud optical thickness from Atmospheric Infrared Sounder (AIRS) measurements," *IEEE Trans Geosci. and Remote Sensing,* vol. 42, pp. 2254-2265, 2004.

[52] M. Wendisch, P. Pilewskie, J. Pommier, S. Howard, P. Yang, A. J. Heymsfield, C. G. Schmitt, D. Baumgardner, and B. Mayer, "Impact of cirrus crystal shape on solar spectral irradiance: A case study for subtropical cirrus," *J. Geophys. Res.,* vol. 110, D03202, doi:10.1029/2004JD005294, 2005.

[53] D. P. Wylie, and W. P. Menzel, "Eight years of high cloud statistics using HIRS," *J. Climate,* vol. 12, pp. 170–184, 1999.

[54] X. Xiong, N. Che, and W. Barnes, "Terra MODIS on-orbit spatial characterization and performance," *IEEE Trans. Geosci. Remote Sens.,* vol. 43, pp. 355-365, 2005.

[55] P. Yang, and K. N. Liou, "Single-scattering properties of complex ice crystals in terrestrial atmosphere," *Contr. Atmos. Phys.,* vol. 71, pp. 223-248, 1998.

[56] P. Yang, B. A. Baum, A. J. Heymsfield, Y. X. Hu, H. L. Huang, S. C. Tsay, and S. Ackerman, "Single-scattering properties of droxtals," *J. Quant. Spectrosc. Radiat.*

Transfer, vol. 79-80, pp. 1159-1180, 2003.

[57] P. Yang, K. N. Liou, K. Wyser, and D. Mitchell, "Parameterization of the scattering and absorption properties of individual ice crystals," *J. Geophys. Res*., vol. 105, pp. 4699-4718, 2000.

[58] P. Yang, S. C. Tsay, H. Wei, G. Guo, and Q. Ji, "Remote sensing of cirrus optical and microphysical properties from ground-based infrared radiometric measurements. Part I: A new retrieval method based on microwindow spectral signature," IEEE Geosci. Remote Sens. Lett., vol. 2, pp. 128-131, 2005.

[59] P. Yang, H. Wei, H. L. Huang, B. A. Baum, Y. X. Hu, G. W. Kattawar, M. I. Mishchenko, and Q. Fu, "Scattering and absorption property database for nonspherical ice particles in the near- through far-infrared spectral region," *Appl. Opt.*, vol. 44, pp. 5512-5523, 2005.

[60] M. H. Zhang, W. Y. Lin, S. A. Klein, J. T. Bacmeister, S. Bony, R. T. Cederwall, A. D. Del Genio, J. J. Hack, N. G. Loeb, U. Lohmann, P. Minnis, I. Musat, R. Pincus, P. Stier, M. J. Suarez, M. J. Webb, J. B. Wu, S. C. Xie, M. S. Yao, and J. H. Zhang, "Comparing clouds and their seasonal variations in 10 atmospheric general circulation models with satellite measurements," *J. Geophys. Res.,* vol. 110, D15S02, doi:10.1029/2004JD005021, 2005.

[61] Z. Zhang, P. Yang, G. W. Kattawar, S. C. Tsay. B. A. Baum, H. L. Huang, Y. X. Hu, A. J. Heymsfield, and J. Reichardt, "Geometric optics solution to light scattering by droxtal ice crystals," *Appl. Opt.,* vol. 43, pp. 2490-2499, 2003.

Ping Yang received the B.S. (theoretical physics) and M.S. (atmospheric physics) degrees from Lanzhou University and Lanzhou Institute of Plateau Atmospheric Physics, Chinese Academy of Sciences, Lanzhou, China, in 1985 and 1988, respectively, and the Ph.D. degree in meteorology from the University of Utah, Salt Lake City, USA, in 1995.

He is currently an Associate Professor in the Department of Atmospheric Sciences, Texas A&M University, College Station, Texas, USA. After graduation from the University of Utah, he remained there for two years, working as a Research Associate. Later, he was an Assistant Research Scientist at the University of California, Los Angeles, and an Associate Research scientist in the Goddard Earth Sciences & Technologies Center, University of Maryland Baltimore County. His research interests cover the areas of remote sensing and radiative transfer. He has been actively conducting research in the modeling of the optical and radiative properties of clouds and aerosols, in particular, cirrus clouds, and their applications to space-borne and ground-based remote sensing. He has co-authored more than 80 peer-reviewed publications. He received a best paper award from the Climate and Radiation Branch, NASA Goddard Space Center in 2000, the U.S. National Science Foundation CAREER award in 2003, and the Dean's Distinguished Achievement Award for Faculty Research, College of Geosciences, Texas A&M University in 2004. He is a member of the MODIS Science Team. He serves as an associate editor for the *Journal of Atmospheric Sciences*, the *Journal of Quantitative Spectroscopy & Radiative Transfer*, and the *Journal of Applied Meteorology and Climatology*.

Lei Zhang received B.S. (meteorology), M.S. and Ph.D. (atmospheric physics) degrees from Lanzhou University, Lanzhou, China in 1982, 1990, and 2001, respectively. He was with the Department of Atmospheric Sciences, Texas A&M University when this study was carried out. He is now a professor and deputy dean of the College of Atmospheric Sciences, Lanzhou University. During the past ten years his research has focused on atmospheric aerosol radiative forcing and its meteorological field response, including

ground-based observation, satellite remote sensing data analysis and numerical simulation with a comprehensive model coupled with four sub-models: a WRF model, an atmospheric diffusion model, an atmospheric radiation transfer model, and an atmospheric boundary layer model.

Gang Hong received the B.S. degree in Atmospheric Sciences from Nanjing Institute of Meteorology, Nanjing, China in 1995 and the Ph.D. degree in Environmental Physics and Remote Sensing from the University of Bremen, Germany in 2004. Currently, he is a Research Associate at the Department of Atmospheric Sciences, Texas A&M University. His recent research focuses on the data analysis and modeling simulation using the MODIS and AIRS measurements.

Shaima L. Nasiri received the B.S. degree in physics and mathematics from the University of Denver in 1997, and the M.S. and Ph.D. degrees in atmospheric sciences from the University of Wisconsin, Madison, in 1999 and 2004, respectively.

She joined the faculty of the Department of Atmospheric Sciences, Texas A&M University in 2006 and is currently an Assistant Professor. Her main research focus is improving the understanding of clouds in the climate system through atmospheric remote sensing and radiative transfer. Recent research has centered on the remote sensing of multilayered clouds and cloud thermodynamic phase.

Bryan A. Baum received his B.S. degree in chemical engineering in 1978 from Vanderbilt University, Nashville, TN, the M.S. degree in chemical engineering in 1985 from the University of Colorado at Boulder, and the Ph.D. degree in atmospheric science in 1989 from the Georgia Institute of Technology, Atlanta, GA.

In 2006, he joined the Space Science and Engineering Center at the University of Wisconsin-Madison as an associate scientist. Prior to this he was a senior scientist at the NASA Langley Research Center for over 16 years. Research activities have focused on

satellite, aircraft, and surface-based remote sensing of single-layered and multilayered cloud properties from multispectral and hyperspectral imager data. Recent research has focused on the development of ice cloud bulk scattering and absorption models at visible through far-infrared wavelengths. He is a member of the MODIS Science Team.

Hung-Lung Huang, also known as Allen Huang, received the B.S. degree in atmospheric science from National Taiwan University in 1984, and the M.S. and Ph.D. degrees in meteorology from the University of Wisconsin, Madison, in 1986 and 1989, respectively.

He joined the Cooperative Institute for Meteorological Satellite Studies (CIMSS) in the Space Science and Engineering Center (SSEC), University of Wisconsin, Madison, in 1989. His research interests include remote sensing in the areas of atmospheric sounding retrieval, information content analysis, satellite and aircraft high-spectral resolution sounding instrument data processing, polar orbiting direct broadcast processing package development, data compression, instrument design and performance analysis, cloud-clearing, cloud property characterization, synergistic imaging, and sounding data processing and algorithm development.

Dr. Huang is a distinguished scientist of University of Wisconsin-Madison, a regional editor of SPIE Journal of Applied Remote Sensing, the US director of China-America Cooperative Remote Sensing Center, Nanjing University of Information and Technology, an adjunct professor of Nanjing University of Information and Technology, the co-chair of International (A)TOVS Working Group, a guest chief scientist of National Satellite Meteorological Center of China Meteorology Administration, a member of International Radiation Commission, a science council member of CIMSS UW-Madison, a council member of SSEC UW-Madison.

Michael D. King (M'01–SM'03) received the B.A. degree in physics from Colorado College, Colorado Springs, in 1971, and the M.S. and Ph.D. degrees in atmospheric sci-

ences from the University of Arizona, Tucson, in 1973 and 1977, respectively.

In January 1978 he joined NASA Goddard Space Flight Center, Greenbelt, MD, and is currently Senior Project Scientist of NASA's Earth Observing System (EOS), a position he has held since 1992. He is a member of the MODIS Science Team where he has primary responsibility for developing the cloud optical and microphysical property and Level-3 algorithms. His research experience includes conceiving, developing, and operating multispectral scanning radiometers from a number of aircraft platforms in field experiments ranging from arctic stratus clouds to smoke from the Kuwait oil fires in the Persian Gulf and biomass burning in Brazil and southern Africa.

Dr. King is a Fellow of the American Geophysical Union and the American Meteorological Society (AMS), and a member of the U.S. National Academy of Engineering. He received the AMS Verner E. Suomi Award for significant and fundamental contributions to remote sensing and radiative transfer, and the IEEE Prize Paper Award.

Steven Platnick received the B.S. degree in electrical engineering from Duke University in 1979, the M.S. degree in electrical engineering from the University of California Berkeley in 1980, and the Ph.D. degree in atmospheric sciences from the University of Arizona in 1991.

He joined NASA Goddard Space Flight Center in January 2003 and is currently Deputy Project Scientist of NASA's *Aqua* satellite. Prior to this appointment, he was a Research Associate Professor in the Joint Center for Earth Systems Technology, University of Maryland Baltimore County, a position he held from 1996-2002. He has worked in collaboration with NASA Goddard Space Flight Center since 1993, and prior to that held engineering positions at Hewlett-Packard Co. for 6 years as well as a National Research Council Resident Research Associate position at NASA Ames Research Center. His research experience includes theoretical and experimental studies of satellite, aircraft,

and ground-based cloud remote sensing, including applications to MODIS. He is a member of the MODIS Science Team.

TABLE 1.

THE ONE-YEAR MEAN MROPERTIES OF HIGH CLOUDS FROM JANUARY 2004 TO DECEMBER 2004 OVER THE TROPICS (30°S–30°N) FROM THE MODIS ONBOARD AQUA IN DAYTIME

High Cloud Properties	Collection 4			Collection 5		
	Land	Ocean	Total	Land	Ocean	Total
Fraction (%)	29.2	22.0	24.0	35.3	21.2	25.1
Optical thickness	14.9	11.4	12.5	14.6	13.3	13.7
Effective radius (μm)	24.1	27.6	26.5	22.2	25.9	24.7
Ice water path (g m^{-2})	219.5	192.4	202.5	198.1	210.6	206.9

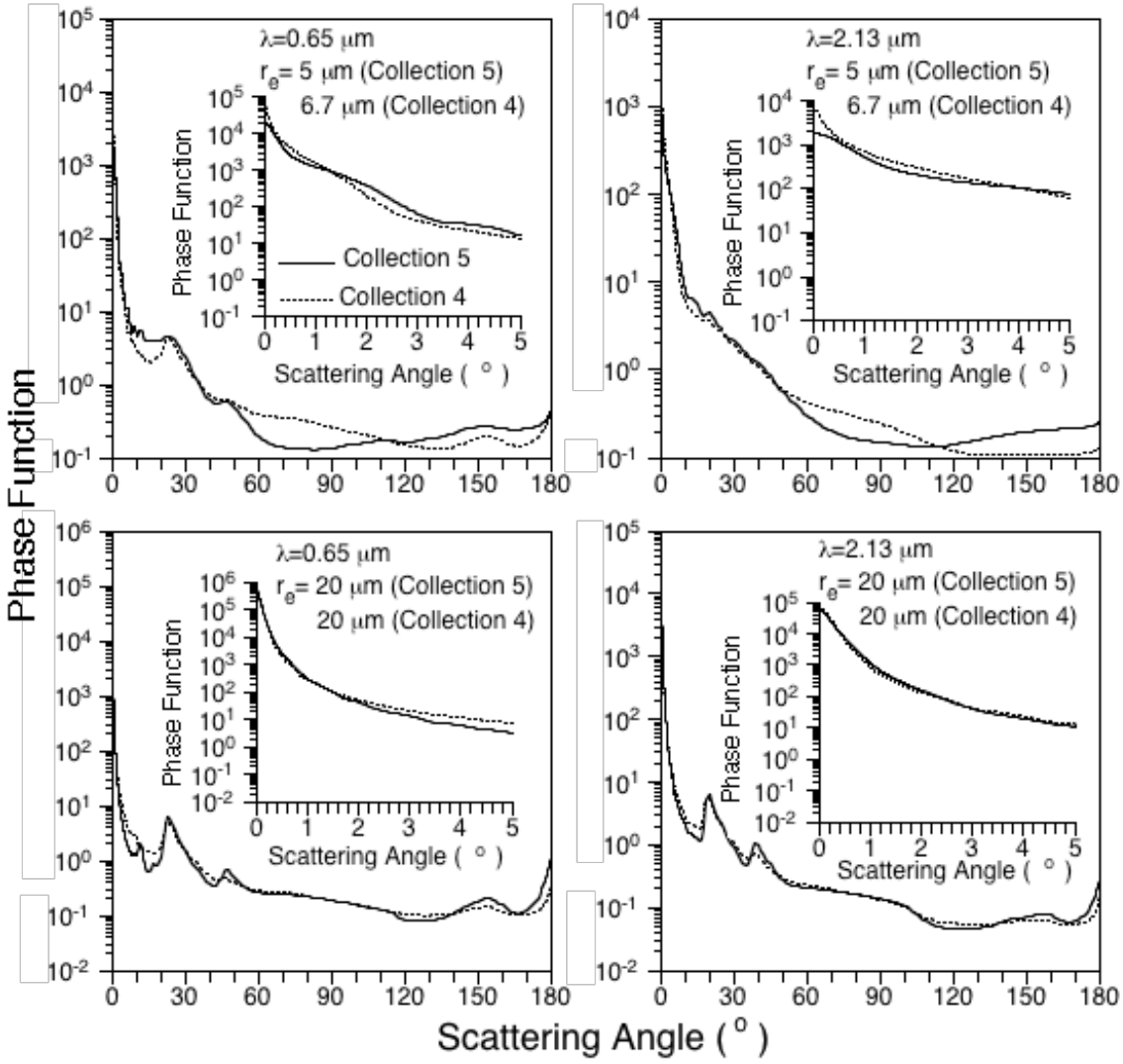

Figure 1. Comparison of the MODIS Collection 4 and 5 scattering phase functions for the MODIS 0.65 and 2.13 μm bands for two values of effective particle radius. The solid and dotted lines indicate Collections 4 and 5, respectively.

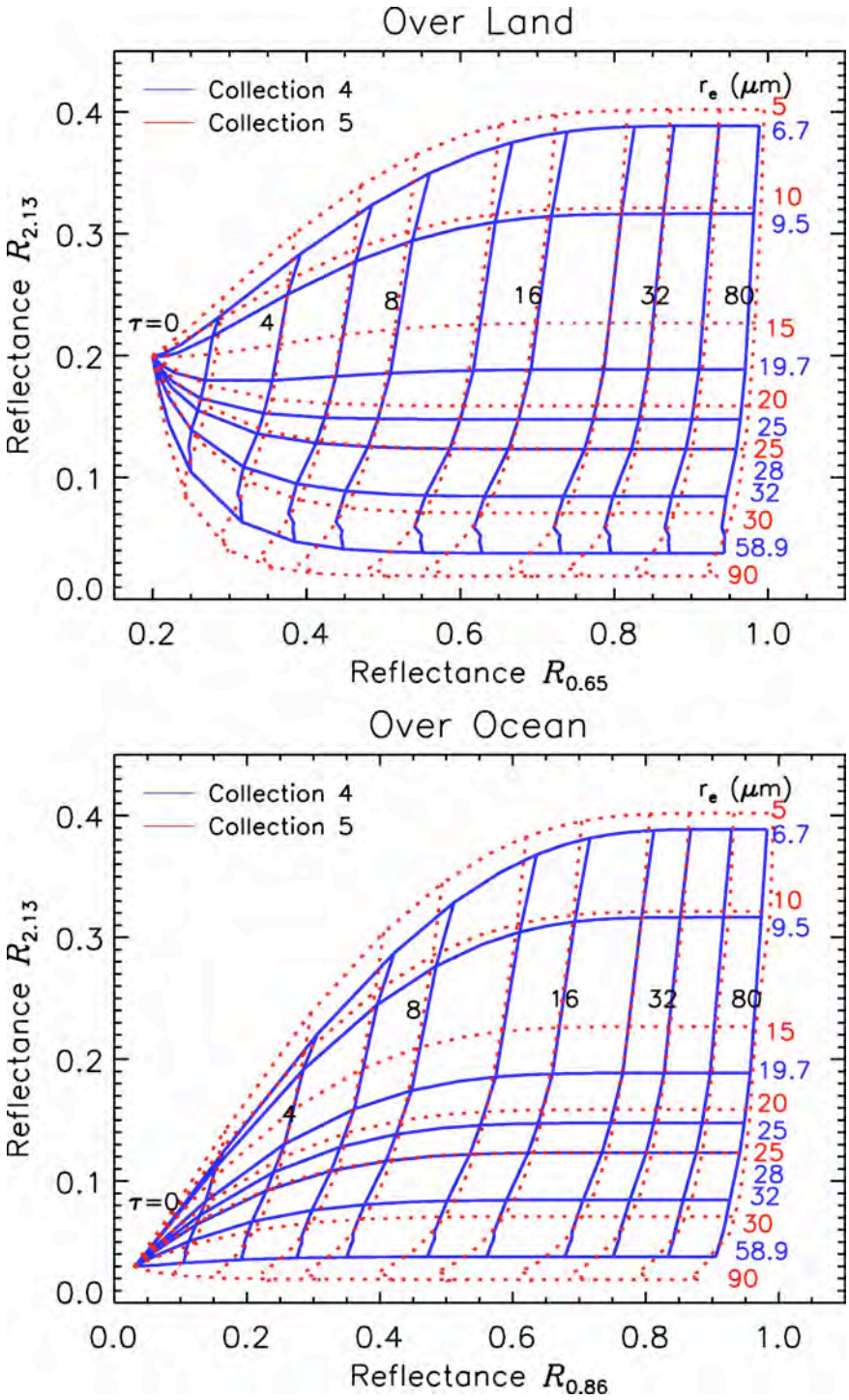

Figure 2. The look-up-tables at 0.65 and 2.13 μm over land and 0.86 and 2.13 μm over ocean for various values of ice cloud optical thickness and effective particle size when $\theta_0 = 30°$ and $\theta = 0°$.

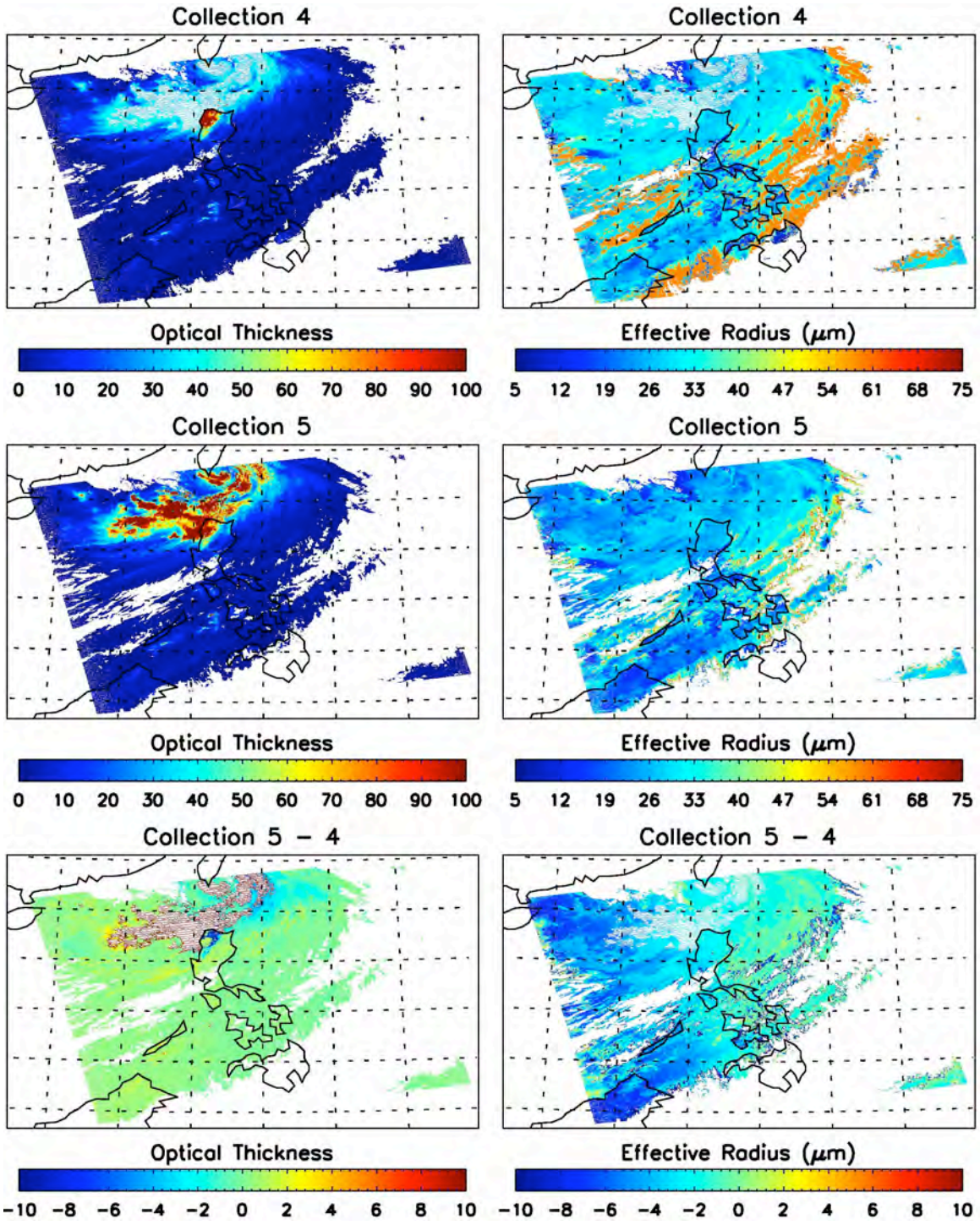

Figure 3. Comparisons of high cloud properties from MODIS Collections 4 and 5 for a granule acquired on July 1, 2004 over Southeast Asia.

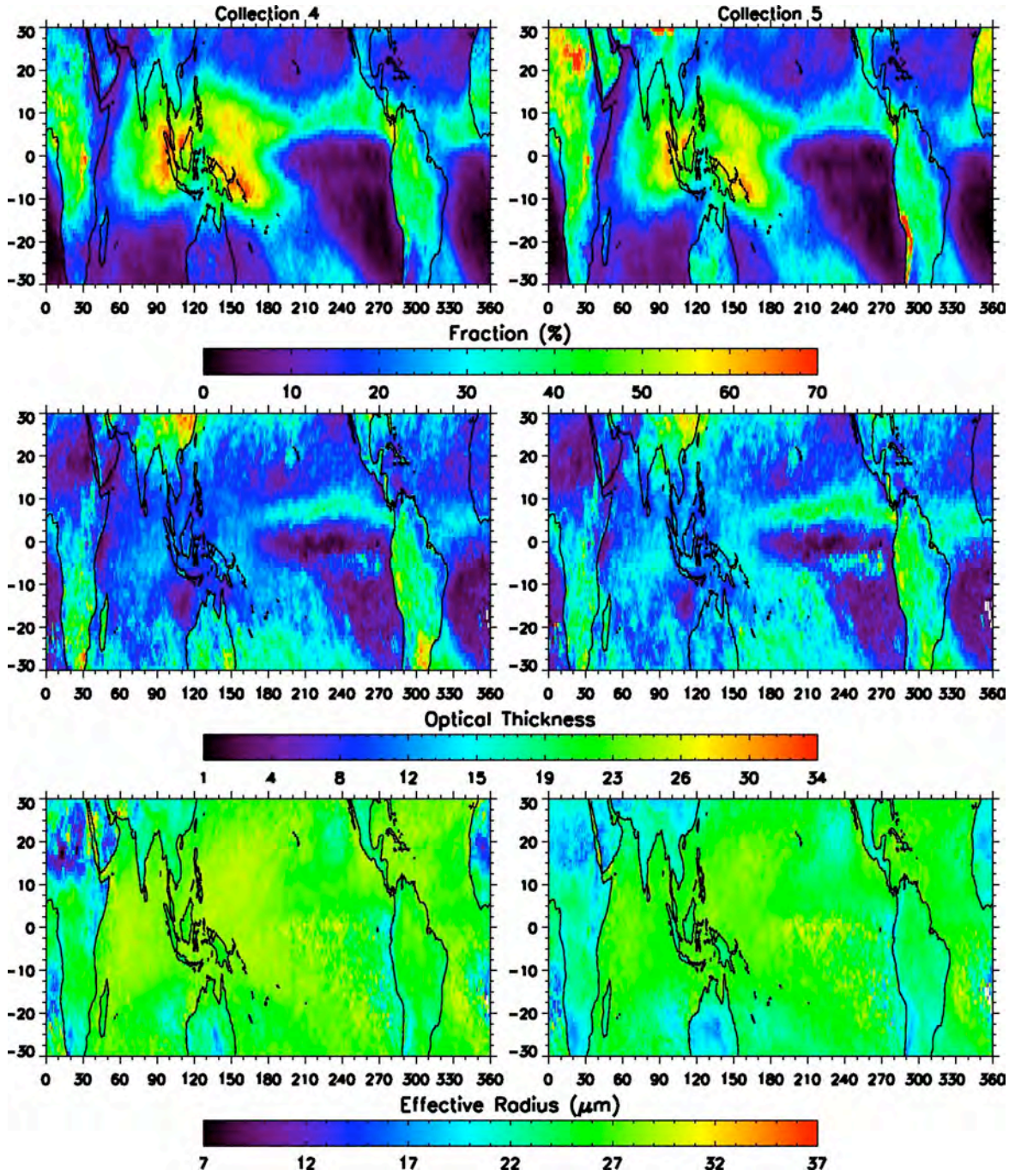

Figure 4. Geographical distributions of high cloud fraction, optical thickness, and effective size over the tropics (30°S–30°N) from Terra MODIS Collections 4 and 5 from January to December 2004.

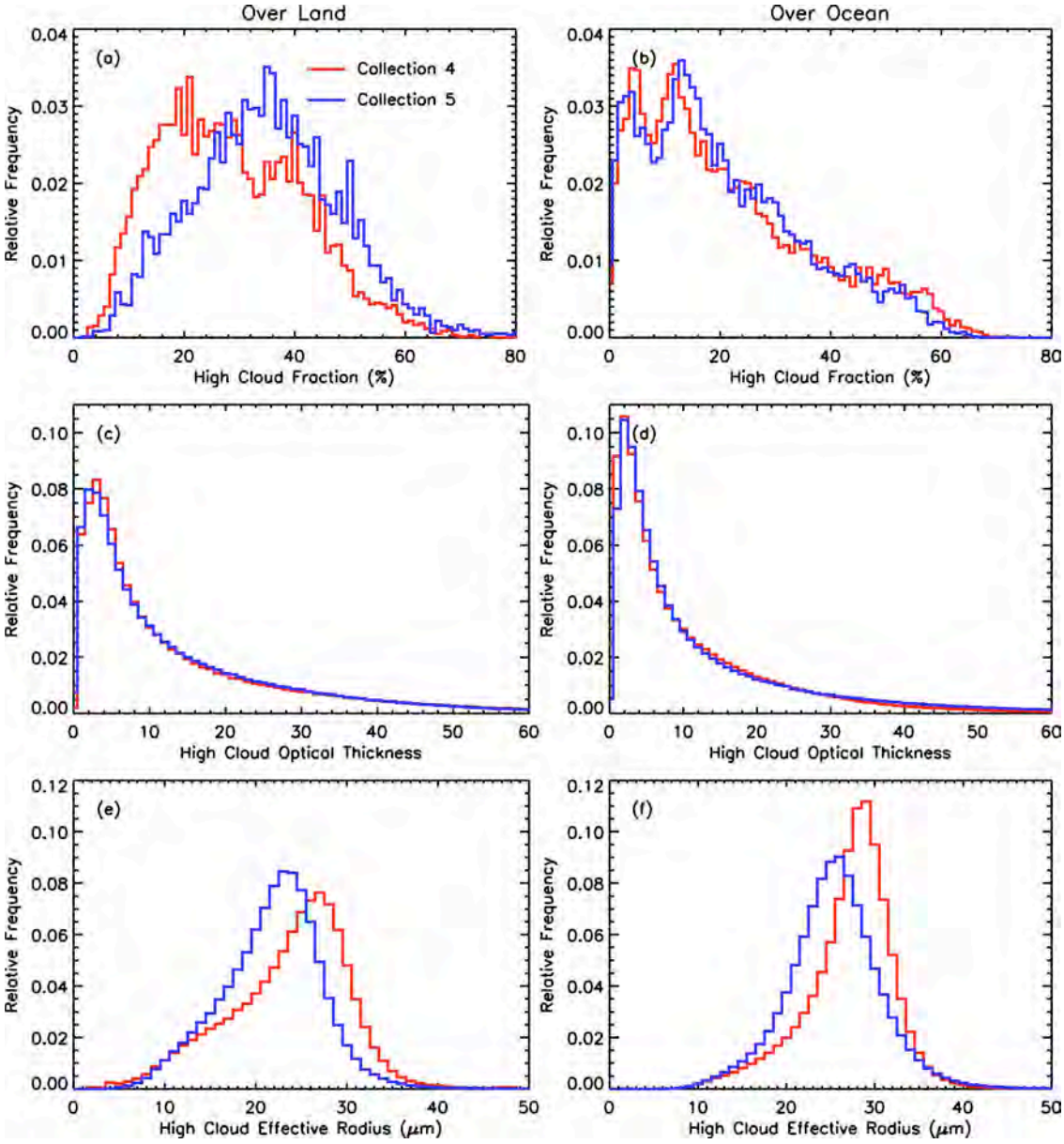

Figure 5. Histogram distributions of high cloud fraction, optical thickness, and effective particle size over ocean and land over the tropics (30°S–30°N) from Terra MODIS Collections 4 and 5 from January to December 2004.

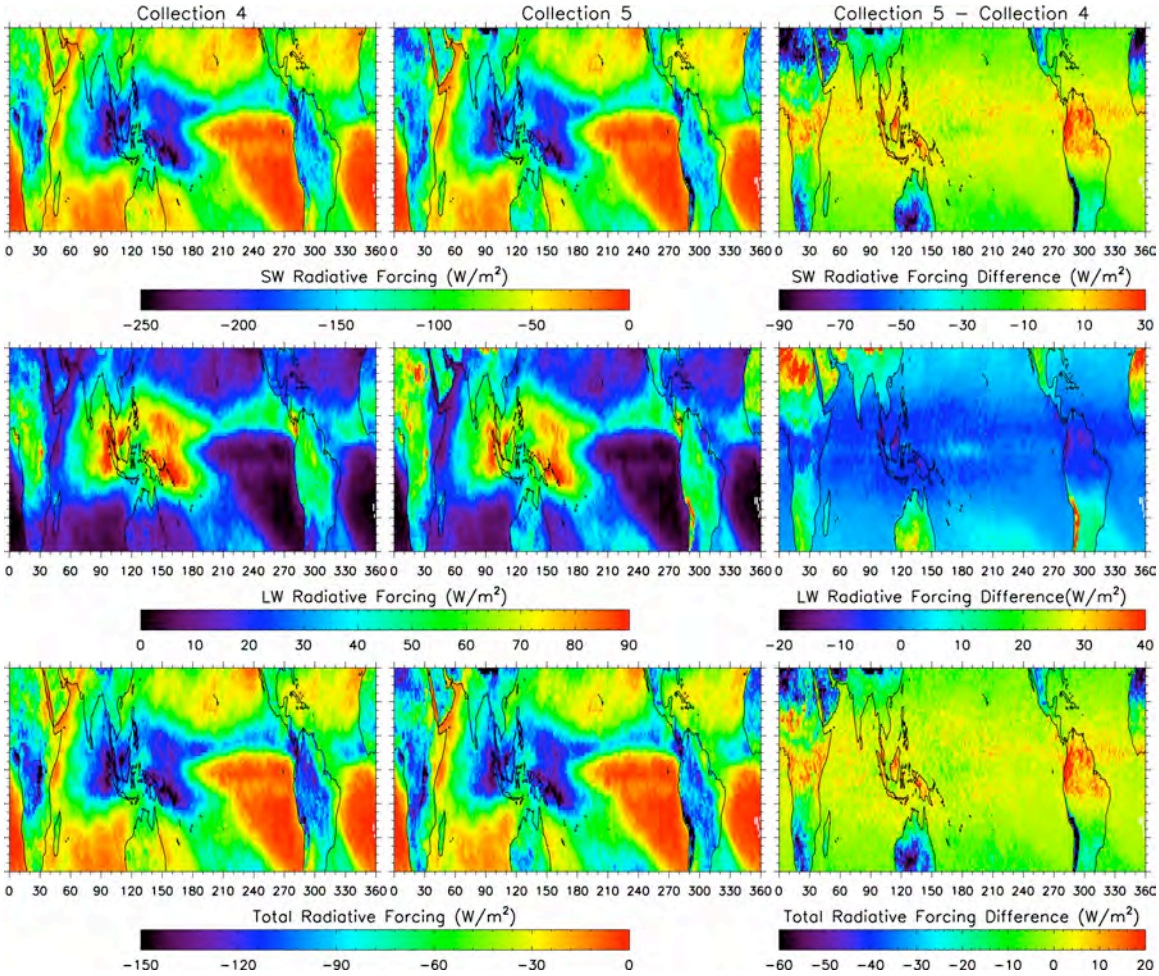

Figure 6. Geographical distributions of ice cloud shortwave (SW), longwave (LW), and total forcing from Collection 4 and 5 and their differences.

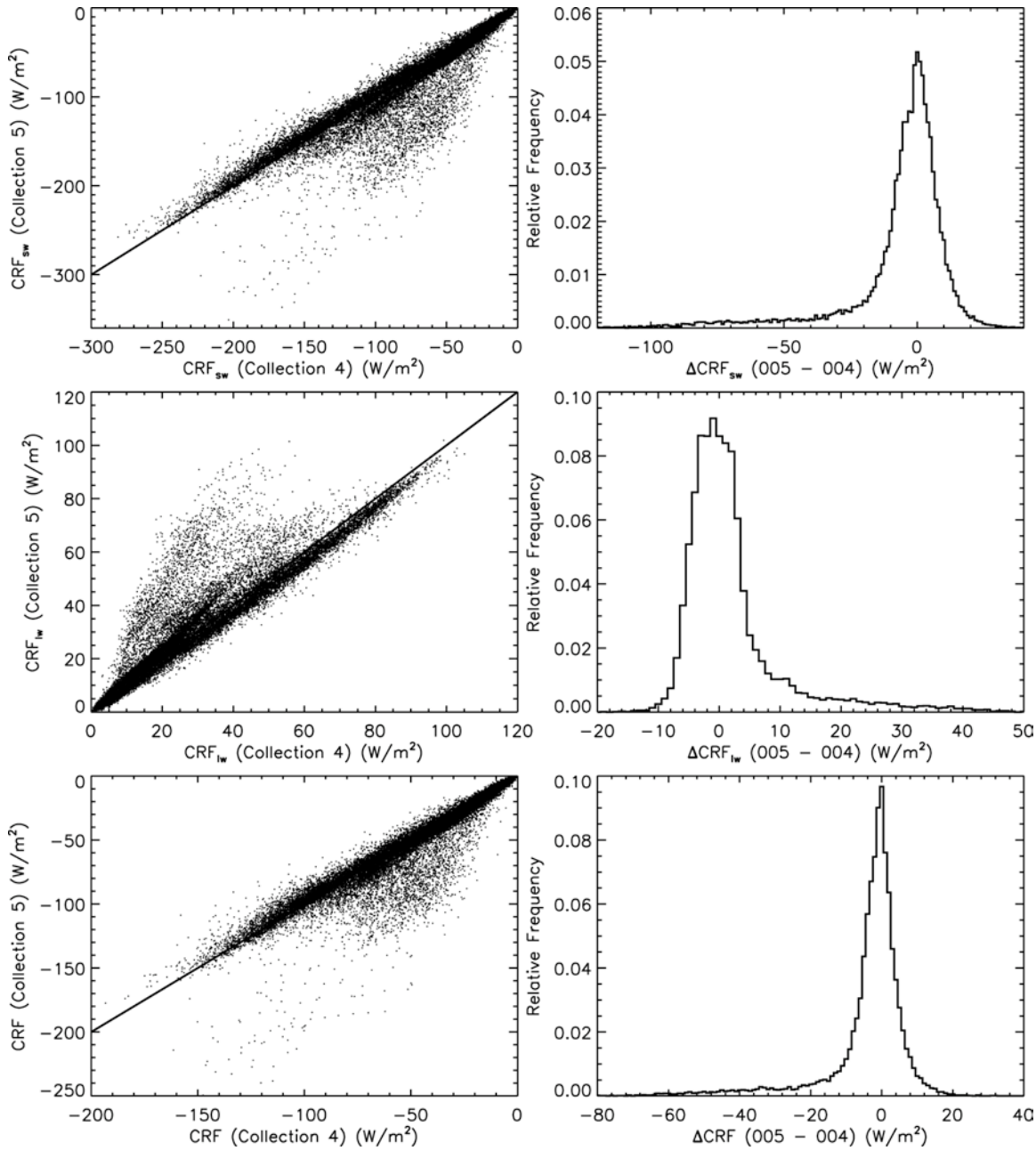

Figure 7. Comparison of ice cloud radiative forcing (CRF_{SW}, CRF_{LW}, and CRF) derived from Collections 4 and 5.

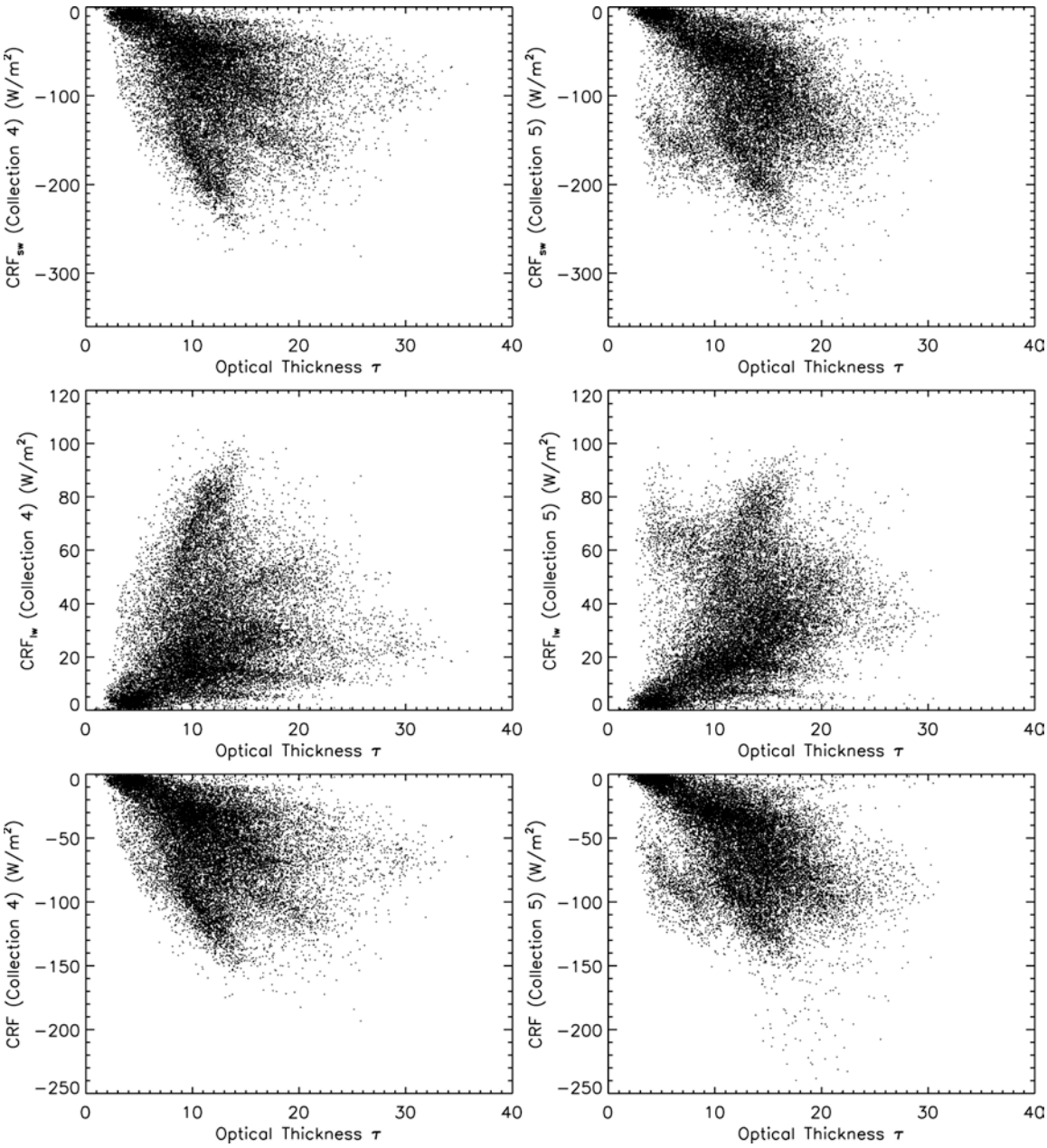

Figure 8. Relationship between ice cloud optical thickness and cloud radiative forcing (CRF_{SW}, CRF_{LW}, and CRF) for Collections 4 (left) and 5 (right).

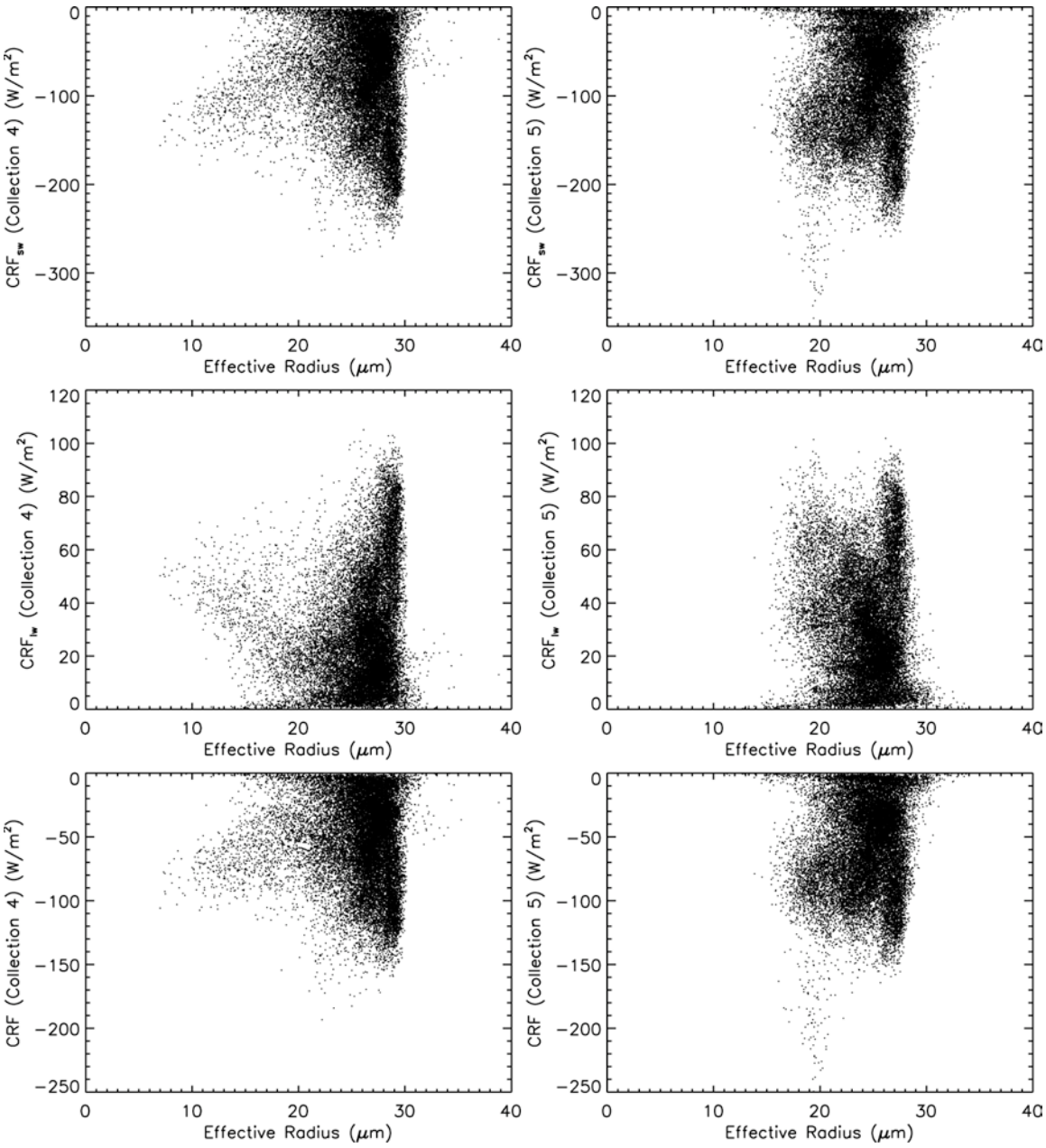

Figure 9. Relationship between ice cloud effective radius and cloud radiative forcing (CRF_{SW}, CRF_{LW}, and CRF) for Collections 4 (left) and 5 (right).